

COVER PAGE

Document downloaded by @DAEL

Thu Nov 26 18:06:51 2026
For personal use

When automatic English translation is provided, only the original document is authentic.
The EAA cannot be held responsible of any translation error

Bibliographical reference

Ultrasonic Velocity Ratio: An Effective Tool for In-Situ Materials Characterization, Anish Kumar, Acta Acustica **vol. 104** (Number 2), 2018, pp. 251-258

DOI
https://doi.org/10.3813/AAA.919167

Acta Acustica united with Acustica
Vol. 104 (2018) 251 – 258

DOI 10.3813/AAA.919167

Ultrasonic Velocity Ratio: An Effective Tool for In-Situ Materials Characterization

Anish Kumar
Metallurgy and Materials Group, Indira Gandhi Centre for Atomic Research, Kalpakkam, Tamil Nadu-603102, India. anish@igcar.gov.in

Summary
Ultrasonic velocity measurements have been widely used for characterization of microstructure, texture and damage in materials. Based on ultrasonic velocity measurements in a wide range of alloy systems and data collected from literature, a new polynomial correlation between velocity ratio and ultrasonic velocity is established for isotropic solid materials. For specific materials/ alloy systems, a linear increase in velocity ratio with increasing ultrasonic shear wave velocity is observed in a wide range of materials. An opposite behaviour to this is observed only for the effect of microcracks/ porosity or pressure/stress on ultrasonic wave velocities. The change in velocity ratio associated with change in ultrasonic velocity is observed in all the cases. Further, as the velocity ratio does not require thickness to be measured physically, it has better potential for in-situ materials characterization applications than ultrasonic velocity. A few applications of velocity ratio for assessment of service induced degradation in materials are also discussed in the paper.

PACS no. 43.20.-f, 43.20.Hq, 43.20.Jr, 43.58.-e, 43.60.-c

1. Introduction

Ultrasonic velocity measurements have been used extensively for characterization of microstructure and mechanical properties in various metallic [1]–[11], non-metallic [12] and ceramic materials [13]–[19]. The basic purpose of ultrasonic velocity measurements have been two fold: (i) to evaluate elastic properties and (ii) to develop ultrasonic velocity measurement based methodology for non-destructive assessment of materials. The elastic properties can be determined with very high accuracy (better than 0.1%) through the measurements of ultrasonic longitudinal V_L and shear/transverse V_T wave velocities and density (ρ) of the material using the following equations:

$$E = \frac{3\rho V_T^2\left(V_L^2 - \frac{4}{3}V_T^2\right)}{V_L^2 - V_T^2}, \tag{1}$$

$$G = \rho V_T^2, \tag{2}$$

$$\nu = \frac{V_L^2 - 2V_T^2}{2\left(V_L^2 - V_T^2\right)} = \frac{1 - 2R_{UV}^2}{2\left(1 - R_{UV}^2\right)}, \tag{3}$$

where $R_{UV} = V_T/V_L$.

The measurement of ultrasonic velocity requires measurement of time of flight (TOF) of ultrasonic wave and thickness of the specimen,

$$\text{Ultrasonic velocity} = \frac{2\times\text{Thickness}}{\text{TOF}}. \tag{4}$$

Received 12 May 2017,
accepted 8 February 2018.

For precise measurement of ultrasonic velocity, the TOF is usually measured with an accuracy of better than ±1 ns using a broad-band ultrasonic transducer and high frequency digitization coupled with advanced signal processing algorithms [1, 7]. The precise measurement (±1 µm) of specimen thickness is usually not an issue for specimens in laboratory for elastic property measurements. This leads to an accuracy of about ±2 m/s in ultrasonic longitudinal wave velocity of 6000 m/s in a 10 mm thick specimen. However, it is often difficult to physically measure thickness in large components or tubes / pipes accurately. It can be obtained from Equation (4) that an error of ±100 µm leads to an error of about ±60 m/s in velocity measurement, which is most often equal to the order of the maximum change in the ultrasonic velocities due to microstructural variations [6]. The extent of error increases further with decrease in thickness. In such cases when thickness cannot be physically measured accurately, either an ultrasonic surface wave based technique (depth information limited by about one wavelength) or ultrasonic velocity ratio ($R_{UV} = V_T/V_L$) based methodology [1, 5, 16] can be employed for materials characterization. For the measurement of R_{UV}, time of flight of ultrasonic longitudinal and shear waves are only required to be measured as shown in Equation (5) below. Hence, it can be precisely measured for in-situ nondestructive materials characterization applications even if thickness of the component cannot be measured.

From Equations (3) and (4):

$$R_{UV} = \frac{V_T}{V_L} = \frac{2\times\text{Thickness}/\text{TOF}_T}{2\times\text{Thickness}/\text{TOF}_L} = \frac{\text{TOF}_L}{\text{TOF}_T}. \tag{5}$$

© S. Hirzel Verlag · EAA

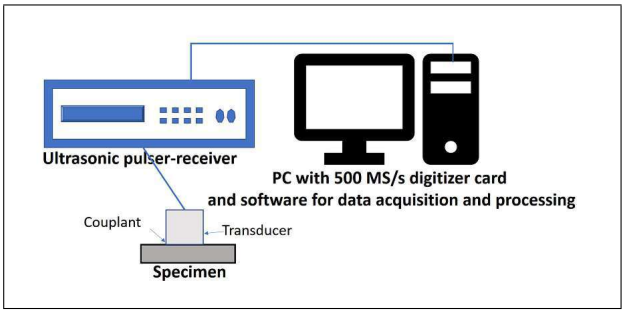

Figure 1. Schematic of the experimental setup for ultrasonic velocity measurements.

Because of the inherent advantage in using the R_{UV} as mentioned above, it has been successfully applied for NDE applications such as for detection of hydride blisters in Zr-2.5 Nb pressure tubes of pressurized heavy water reactors [8], characterization of hydrogen damage in steels [20], and for characterization of porosity in rocks [16] and other ceramic materials [17]. Alternatively, Poisson's ratio derived from the R_{UV}, as per Equation (3), has also been used for various applications such as for measurement of volume fraction of different phases in alloys [1, 2, 4, 6, 7], assessment of degradation in Inconel 625 ammonia cracker tubes due to precipitation of intermetallic phases [5] and assessment of creep damage in silicon nitride [17]. Since R_{UV} depends upon Poisson's ratio (varies inversely), the sensitivity of R_{UV} for materials characterization would solely depend upon the sensitivity of Poisson's ratio to the microstructural variations. Poisson's ratio, the ratio of the lateral contraction to the longitudinal expansion, is reported to provide more information about the character of the bonding forces than any of the other elastic coefficients [21]. Kumar *et al.* [6] established a new correlation between ultrasonic shear wave velocity and Poisson's ratio for isotropic solid materials. It was observed that Poisson's ratio decreases with increasing ultrasonic velocity in various pore-free solid materials such as metals and alloys, ceramics and glasses, intermetallics and polymers. This also indicates increase in R_{UV} with increasing ultrasonic velocities for isotropic solid materials, as Poisson's ratio and R_{UV} varies inversely (as per Equation 3). Inverse relationship between R_{UV} and ultrasonic velocities (decrease in R_{UV} with increasing ultrasonic velocities) have been observed only for materials with presence of voids [13, 16, 18] / micro-cracks [20, 22] or application of pressure [23] / stress [24, 25].

The present study explores the utility of R_{UV} for in-situ nondestructive microstructural characterization in a wide range of materials. As ultrasonic velocities have been widely used for materials characterization applications, correlation between R_{UV} and an ultrasonic velocity has been first attempted to study the sensitivity of R_{UV} for microstructural characterization. The results are discussed separately for two different cases: (a) Case I- for isotropic solid materials, where R_{UV} increases with increasing ultrasonic velocities and (b) Case II- for materials with pores/microcracks or effect of pressure/ stress on ultrasonic velocities, where R_{UV} decreases with increasing ultrasonic velocities. A new polynomial relationship is derived for increase in R_{UV} with increasing ultrasonic velocity for a wide range of isotropic solid materials (Case-I), based on the experimentally generated data and those collected from the literature. Further, variation in R_{UV} with ultrasonic velocity is analyzed for specific alloy systems. As the measurement of R_{UV} doesn't require thickness to be measured physically unlike ultrasonic velocity, the application of R_{UV} for in-situ characterization of degradation in mechanical properties in Inconel 625 ammonia crack tubes is demonstrated. A few examples of Case-II are also discussed including characterization of hydrogen damage in boiler water tubes of power plants, assessment of depth of inter-granular corrosion (IGC) damage in a stainless steel and effect of stress on R_{UV} and ultrasonic velocities.

2. Data generation/compilation

A part of the results discussed in the present study is generated experimentally in the author's laboratory and the rest of the data are collected from literature. The experimental details used in the author's laboratory for measurement of time of flights of ultrasonic waves are described in Section 2.1.

2.1. Experimental details

The typical experimental setup used for ultrasonic velocity measurements performed in the author's laboratory is depicted in Figure 1. Ultrasonic velocities were measured using 5 MHz (/2.5 MHz) shear and 15 MHz (/5 MHz) longitudinal wave normal beam transducers, to keep the wavelength almost similar in both the ultrasonic wave modes. Normal beam shear wave measurements require a viscous couplant to be used for transmission of shear waves. Hence, honey was used as a couplant for both shear wave and longitudinal wave measurements. The specimens' lateral dimensions and thickness were much larger than the wavelength to allow all the measurements in true bulk wave conditions. Hence, the changes in ultrasonic velocities analyzed in the paper can solely be attributed to the microstructural/ physical changes. A broad-band pulser-receiver was used to pulse, receive and amplify the ultrasonic signals. The signals were digitized using a 500 MHz PCI based digitizer card (/oscilloscope) and precise measurement of ultrasonic velocities were performed using a cross-correlation based algorithm developed in LabVIEW [1, 7]. The cross-correlation based algorithm was adopted as it is reported to provide better precision [26], even for conditions with poor signal to noise ratio [27]. The algorithm comprises of spline fitting near the maximum peak of the cross-correlation function and its interpolation to obtain an accuracy of better than the sampling step of 2 ns in time of flight measurements. The maximum scatters in the measurement of ultrasonic longitudinal and shear wave velocities are found to be ±2.5 m/s and ±1.5 m/s respectively and the corresponding maximum scatter in R_{UV} is

Table I. Microstructural variations studied in different alloys and corresponding range of variations in ultrasonic velocity and ultrasonic velocity ratio. Ultrasonic velocities could not be measured in Inconel 625 ammonia cracker tubes and boiler water tubes due to lack of thickness values.

Sl.No.	Materials	Microstructural variations	Range shear velocity	Range of R_{UV}	Reference
1	Ferritic steels	Vol.fraction of ferrite and martensite	3272–3310	0.5500–0.5519	[10]
2	Maraging steel	Precipitation of intermetallic phases	2853–3000	0.5104–0.5248	[4]
3	$\alpha+\beta$ and β-Ti-alloys	Vol.fraction of different phases	2570–2967	0.4546–0.4978	[1, 3, 7]
4	Zr-base metallic glass	Recrystallization of metallic galss	2443–2936	0.4752–0.5303	[2]
5	Inconel 625	Precipitation of intermetallics	–	0.5152–0.5389	[5, 9]
6	Boiler water tube	Hydrogen damage	–	0.5411–0.5964	–

$\sim \pm 0.00025$. The maximum scatter in the measurement of ultrasonic velocity and velocity ratio mentioned above are the maximum variations observed in the parameters by repetitive measurements at the same location. The scatter inherently includes the variations in coupling condition in different measurements. The error in time of flight measurement due to coupling condition in properly performed ultrasonic measurements on machined surfaces is reported to be less than 1 ns [28], which is smaller than the maximum variation considered in the present paper in different measurements. Further, error due to slight surface roughness or couplant variation will have less effect on velocity ratio as compared to the absolute velocity. Hence, the effect of coupling is not discussed specifically in the present paper.

Table I lists the microstructural variations studied in a range of metallic materials for studying the variation in velocity ratio with ultrasonic velocities, in the author's laboratory. The detailed microstructural information can be obtained in the references cited in the last column. The velocity ratio based methodology has been implemented for assessment of in- service degradation in mechanical properties of Inconel 625 ammonia cracker tubes in Heavy Water Plants at Thal and Tuticorin, India [5]. TOFs of ultrasonic longitudinal and shear waves were measured in-situ on the cracker tubes of 8.95 mm wall thickness, 88 mm outer diameter and 12.55 m length. Hardness measurements, using a hand held portable hardness tester EQUITIP 2 (Proceq Testing Equipments, Switzerland), were also carried out to correlate with the ultrasonic measurements. Ultrasonic measurements were performed in virgin tubes (unused/ fresh tubes in solution annealed condition), tubes exposed for 750 h and 120,000 h (taken out of Cracker unit for re-solution annealing) and re-solution annealed (RSA) tubes (RSA after 120000 h of service exposure). All the measurements were carried out at 1 m elevation from the bottom weld. R_{UV} measurements were also performed on a few boiler water tubes (made of medium carbon steel) failed due to hydrogen damage. The R_{UV} in the damaged (fired) and un-damaged (back) sides of the tubes are compared for different tubes.

2.2. Data collected from literature

In addition to the data listed in Table I, the ultrasonic velocities and R_{UV} values were also collected from the literature and suitably cited in the manuscript. Out of the data collected from the literature, data for various isotropic materials are obtained from [6] and the references to the original sources are provided therein. For examples of Case II, the effect of IGC damage in a stainless steel [22], effect of pressure on metallic materials [23] and effect of stress in steels [24] are obtained from literature, as cited.

3. Results and Discussion

From the first law of thermodynamics, it can be seen that E, B and G are positive and since $B = E/[3(1-2\nu)]$ and $G = E/[2(1+\nu)]$, it follows that $-1 < \nu < 0.5$ [6, 29]. Further, even though, the laws of thermodynamics are not violated by a hypothetical isotropic elastic solid with $-1 < \nu \leq 0$, such negative values of ν have been only observed in foam structures and anisotropic materials [30]. Thus, in isotropic solids, ν is bounded practically by 0 and 0.5. Considering these limits of ν, the limits of R_{UV} can be obtained using

$$R_{UV} = \sqrt{\frac{2\nu - 1}{2(\nu - 1)}}. \tag{6}$$

For $\nu = 0$, $R_{UV} = 0.707$ and for $\nu = 0.5$, $R_{UV} = 0$. $R_{UV} = 0$ corresponds to $V_T = 0$. Hence, the bounds of R_{UV} are 0 ($V_T = 0$) and 0.707. These indicate that R_{UV} is minimum for $V_T = 0$.

The variation in ν or R_{UV} with ultrasonic velocities can be analyzed by differentiating the relationship of ν with V_L and V_T (Equation 3) [6],

$$\frac{\mathrm{d}\nu}{\nu} = \frac{2V_L^2 V_T^2}{(V_L^2 - V_T^2)(V_L^2 - 2V_T^2)} \left(\frac{\mathrm{d}V_L}{V_L} - \frac{\mathrm{d}V_T}{V_T} \right). \tag{7}$$

It can be seen from Equation (7) that the variation in Poisson's ratio would depend upon the relative variations in V_L and V_T. Further, with any change that occurs in the material, V_L and V_T, tend to respond in the same direction (increase or decrease). Hence, it is difficult to deduce from Equation (7), that whether the variation of ν or R_{UV}, due to the metallurgical or physical changes, would be in the same or opposite direction to the ultrasonic velocities. The nature of the variation of ν would therefore depend upon the fact that which one among the V_L and V_T is affected

more by metallurgical variables. If the relative change in V_T is more than that in V_L, then the right-hand side of Equation (7) will be negative and hence ν will vary opposite to those of V_L and V_T. Similarly, when the relative change in V_L is more than that in V_T, the right-hand side of Equation (7) will be positive and hence ν will vary in line with V_L and V_T. These two conditions are discussed separately as Case I and Case II in Sections 3.1 and 3.2, respectively.

3.1. Case I: Increasing R_{UV} with ultrasonic velocities

Variations in R_{UV} with ultrasonic shear wave velocity are shown in Figure 2 for a wide range of isotropic solid materials including metals and alloys, bulk metallic glasses, polymers and ceramics. The data shown in Table I and those reported in [6] are plotted in Figure 2. The limits of R_{UV} are also shown in Figure 2 as dotted lines. The minimum and the maximum experimental values of R_{UV} have been reported for Pb and Be as 0.32 and 0.70, respectively [6]. The variation in R_{UV} with shear wave velocity can be expressed as a simple polynomial equation as shown in Equation (8):

$$R_{UV} = 0.08 V_T^{0.2}, \tag{8}$$

$$\frac{\mathrm{d}R_{UV}}{\mathrm{d}V_T} = \frac{0.02}{V_T^{0.76}}. \tag{9}$$

It can be seen from Equations (8) and (9) that the rate of change in R_{UV} decreases with increasing V_T. This indicates that for a small change in V_T, a large change in R_{UV} and thus in Poisson's ratio (Equation 3) is expected for materials with lower V_T values such as heavy metals, rubber, polymers etc. as compared to materials with higher V_T values such as ceramics and light metals. This also indicates that R_{UV} will be a more effective parameter for characterization of polymers and metals as compared to ceramics.

3.1.1. Microstructural characterization in specific alloy systems

The variations in R_{UV} with ultrasonic shear wave velocity for specific alloy systems for which measurements are performed in the author's laboratory are shown in Figure 3. The specimens with different ultrasonic velocities were obtained by altering microstructure by employing suitable heat treatments as indicated in Table 1 and detailed in the references given therein. For example, specimens with various volume fractions of different phases in ferritic steel [10] and titanium alloys [1, 7] were generated by subjecting the specimens to heat treatments at different temperatures followed by quenching in oil and water, respectively. In addition, the data corresponding to the influence of temperature on various pure metals [29] are also shown in Figure 3. The data corresponding to the effect of heat treatment on ultrasonic velocities in a Pd-based bulk metallic glass [11] are also included. It can be observed that with microstructural changes in all the alloy systems, R_{UV} increases with increasing ultrasonic velocities. For

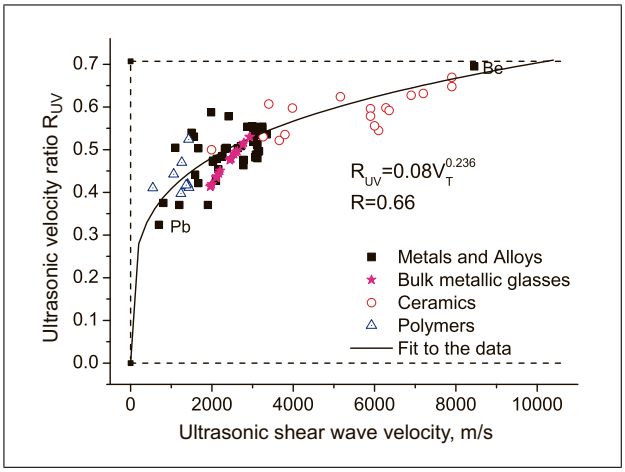

Figure 2. Variation in ultrasonic velocity ratio with ultrasonic shear wave velocity.

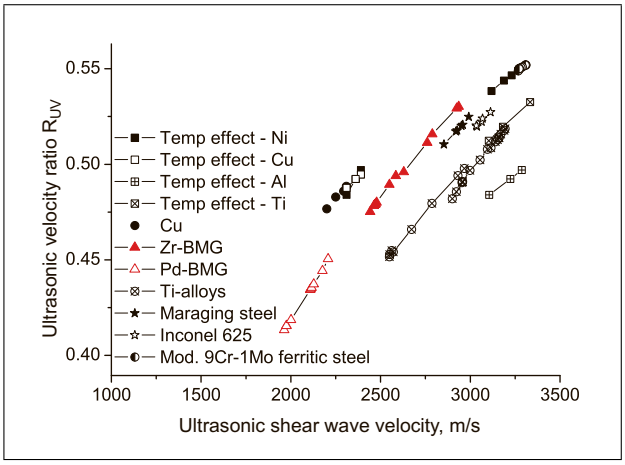

Figure 3. Variation in ultrasonic velocity ratio with ultrasonic shear wave velocity in specific alloy systems.

the limited range of R_{UV} and V_T observed in a given alloy system, a linear correlation can be obtained as

$$R_{UV} = C + 1.027 \cdot 10^{-4} V_T, \tag{10}$$

where C is a constant depending upon the specific alloy system.

It can be seen in Figure 3 that the slopes are almost similar for all the alloy systems and the slope exhibits steeper change in R_{UV} as compared to that obtained from the correlation shown in Figure 2 and Equation (9). The largest variation in ultrasonic parameters are observed in bulk metallic glasses (BMG) and Ti-alloys. The ultrasonic parameters (both R_{UV} and V_T) exhibit minimum values in the as cast BMG and increase with the extent of recrystallization [2, 11]. In case of Ti-alloys, the ultrasonic parameters decrease with increasing volume fraction of beta phase [1, 3, 7]. A linear correlation between ultrasonic velocities and volume fraction of alpha/beta phase was observed in a beta-Ti alloy for a range of volume fraction of alpha phase from 0–50% obtained with heat treatment at different temperatures [1]. In modified 9Cr-1Mo ferritic steel, ultrasonic parameters decreased with

increasing heat treatment temperature in the intercritical temperature region (alpha+austenite phase region) due to increasing volume fraction of martensite phase upon quenching [10]. In M250 maraging steel, ultrasonic parameters increased with increasing precipitation of intermetallic phases (Ni_3Ti and Fe_2Mo) [4].

3.1.2. In-situ assessment of degradation in Inconel 625 ammonia cracker tubes using R_{UV}

In a nickel base alloy Inconel 625 used as ammonia cracker tubes in heavy water plants, ultrasonic parameters were found to increase with precipitation of intermetallic phases ($Ni_2(Cr, Mo)$ and γ") during long term exposure to intermediate temperature (∼873 K) and decrease with their dissolution during resolution annealing [9]. Inconel 625 is used in ammonia cracker tubes in the solution treated condition. In this condition, the yield strength is minimum (370 MPa) and the ductility is maximum (∼60% uniform elongation). With the precipitation of interrmetallic phases during service exposure, yield strength increases to about 1000 MPa along with drop in ductility to about 6% uniform elongation. It is important to evaluate the extent of degradation in mechanical properties of the cracker tubes nondestructively, so that they can be subjected to solution heat treatment to regain their mechanical properties and thus any failure due to brittleness of the tube can be avoided [5].

Ultrasonic velocity measurements performed on the service exposed and post-service heat treated specimens exhibited that the ultrasonic velocities were minimum in the solution annealed condition and increased with the precipitation of intermetallic phases. However, due to the tube geometry, it was not possible to measure thickness at the locations of ultrasonic measurements. Thus, the absolute values of ultrasonic velocities couldn't be measured for nondestructive assessment of the tube. However, it can be seen from Figure 3 that any change in ultrasonic velocity due to microstructural changes is always associated with a change in R_{UV} also and measurement of R_{UV} doesn't require thickness to be measured. Hence, the TOFs of ultrasonic longitudinal and shear waves were measured at the same locations to obtain R_{UV} in tubes exposed to different service conditions. Figure 4 shows the variations in R_{UV} with in-situ measured surface hardness values. It can be seen that the R_{UV} exhibit minimum values in the virgin/ resolution annealed conditions and it increases with increasing hardness upon service exposure. A large range of R_{UV} / hardness values are observed in the tubes exposed to 120,000 h of service, when they were removed for resolution annealing treatment. Thus, even though the tubes were subjected to similar duration of service exposure, the extent of degradation were not the same in different tubes. The scatter in the correlation of R_{UV} with hardness may be attributed to the fact that different intermetallic precipitates affect the correlation between elastic and plastic properties differently depending upon their chemical composition and coherency strain induced by them [9]. The study clearly demonstrates the capability of R_{UV} for in-situ applications for assessment of service induced degradation

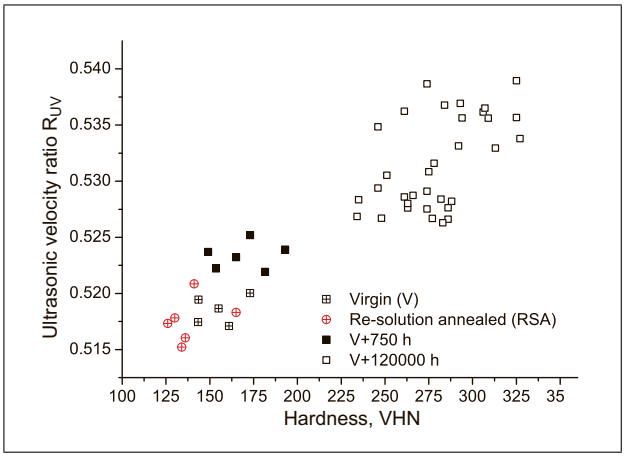

Figure 4. Variation in ultrasonic velocity ratio with hardness for Inconel 625 ammonia crack tubes in different service conditions.

in materials properties, where ultrasonic velocities cannot be measured precisely due to the difficultly in measuring the thickness of the components.

3.2. Case II: Decreasing R_{UV} with increasing ultrasonic velocities

The above examples in Section 3.1 are shown for pore-free isotopic solid materials. In all such materials, increasing R_{UV} is observed with increasing ultrasonic velocities. The opposite behavior to this is reported by many authors in porous materials [13, 16, 18] and materials with microcracks [17]. Decrease in ultrasonic velocities are observed with increasing porosity. Most of the reports indicate more relative change in ultrasonic longitudinal wave velocity as compared to the shear wave velocity with increasing porosity. In other words, increase in R_{UV} / decrease in Poisson's ratio is reported with increasing porosity [13, 16, 17, 18]. Similar behaviour is also observed in the case of service induced degradation in materials properties associated with generation of microcracks. Generation of microcracks lead to decrease in ultrasonic velocities. An increase in R_{UV} with increasing extent of creep damage in SiN specimens are reported [17]. Increase in R_{UV} is also reported with hydrogen damage induced micro cracking in ferritic steel tubes [20].

3.2.1. Hydrogen damage in boiler water tubes

Boiler water tubes in power plants are made of medium carbon steel. Steam is generated inside these tubes by firing from one surface side. These tubes are susceptible to microcracking due to hydrogen damage on fire side surface during the service. This is usually a localized damage spreading over a small circumferential range directly facing the fire. In most of the cases, reduction in wall thickness is also associated with hydrogen damage. Hence, even though, reduction in ultrasonic velocities are expected due to hydrogen damage, they cannot be implemented for assessment of hydrogen damage due to varying thickness and difficulty in measuring thickness in the tubes. Hence, R_{UV} measurements have been performed in

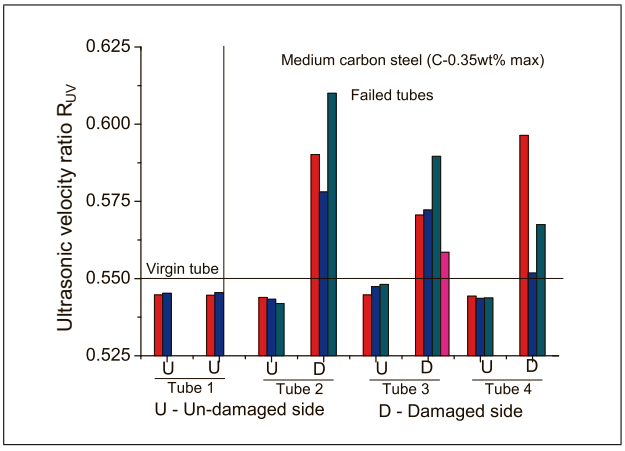

Figure 5. Variations in ultrasonic velocity ratio at different locations in a virgin tube and on the undamaged (U) and hydrogen damaged (D) sides in three failed tubes.

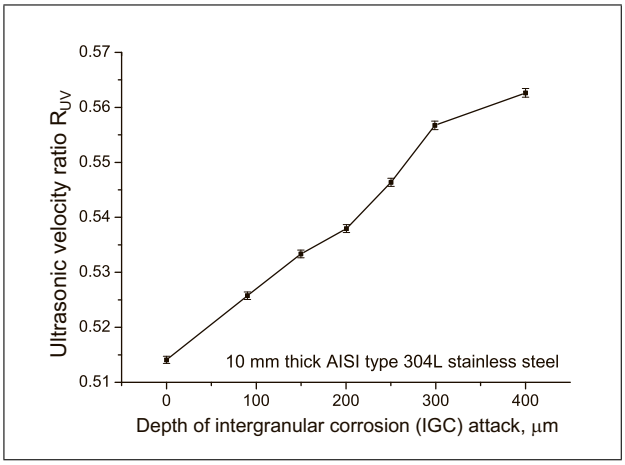

Figure 6. Variation in ultrasonic velocity ratio with depth of inter–granular corrosion attack in a 10 mm thick AISI type 304L austenitic stainless steel.

a few tubes failed due to hydrogen damage in a power plant to explore the feasibility of using R_{UV} for in-situ damage assessment. The hydrogen damage is expected to be only on the side of the tube exposed to the fire side. Figure 5 shows the R_{UV} values obtained at different locations in a virgin tube (Tube 1) and three tubes (Tubes 2–4) failed due to hydrogen damage. To study the variation across the length of the tube, measurements were performed at different locations as reported in Figure 5. The R_{UV} values in the virgin tube are about 0.54 on both the sides. In the hydrogen damaged tubes also, the R_{UV} values are found to be less than 0.55 at all the locations on the undamaged side (opposite to the fire side). However, R_{UV} values of more than 0.55 is observed at different locations (indicated by different colors in Figure 5) in the damaged side in all the three tubes. The different R_{UV} values on the fire side indicate different extent of hydrogen damage in the tubes at different locations. The study indicates that R_{UV} can be effectively used for in-situ assessment of hydrogen damage in boiler water tubes.

3.2.2. Assessment of inter-granular corrosion in stainless steel

Another corrosion mechanism causing microcracking is the inter-granular corrosion (IGC). Jothilakshmi *et al.* [22] have used ultrasonic velocities and velocity ratio for characterization of IGC damage in an AISI type 304L austenitic stainless steel. They have correlated V_L/V_T with the depth of IGC damage. To maintain uniformity in this paper, R_{UV} $(= V_T/V_L)$ is calculated from the data reported by them. Figure 6 shows the variation in R_{UV} with depth of inter-granular corrosion attack in a 10 mm thick AISI type 304L austenitic stainless steel. Similar to that observed in the case of hydrogen attack, an increase in R_{UV} is observed with increasing depth of microcracking. Increased depth of microcracking is expected to decrease ultrasonic velocity [22]. Hence, increase in R_{UV} is observed with decreasing ultrasonic velocity in this case also due to changes associated with the presence of microcracks.

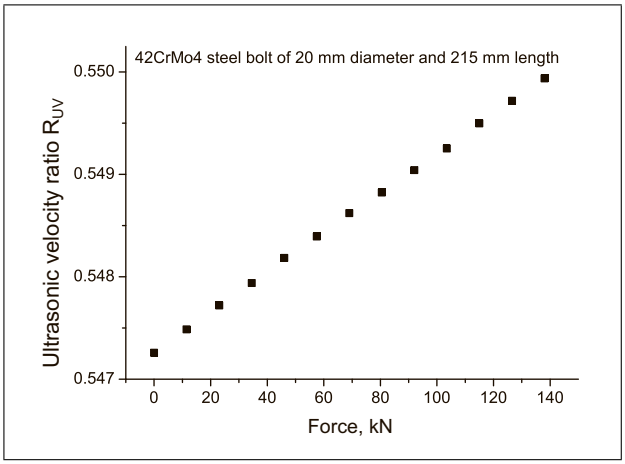

Figure 7. Variation in ultrasonic velocity ratio with tightening load in 42CrMo4 steel bolt of 20 mm diameter and about 215 mm length.

3.2.3. Influence of stress on R_{UV}

Other than the presence of pores/microcracks, pressure/stress is the only factor which has been systematically reported to cause opposite effects on R_{UV} and ultrasonic velocities [23, 24, 25]. Reduction in ultrasonic velocity with increasing tightening force is reported by many authors due to the acoustoelastic effect [24, 25]. Further, a linear increase in the velocity ratio (V_T/V_L) has been observed with increasing tightening load in a 42CrMo4 steel bolt of 20 mm diameter and about 215 mm length, as shown in Figure 7 [24]. Chaki *et al.* [24] reported variations in V_L/V_T with the tightening load. To maintain uniformity in this paper, R_{UV} $(= V_T/V_L)$ is calculated from the data reported by them. Even though the change due to the acoustoelastic effect is very small as compared to the other microstructural changes (Figures 2–6), a precise measurement of time of flight of ultrasonic longitudinal and shear waves provides systematic variation in R_{UV} with tightening load.

It can be observed from the above described case studies that except for the cases related to the direct volumetric effects (pores/microcracks or pressure/stress), R_{UV} increases with increasing ultrasonic velocities. From Equation (7), this indicates that the relative change in shear wave velocity is always more than that in the longitudinal wave velocity for any change in microstructure of a material, except for the effects associated with pores/microcracks or pressure/stress.

4. Conclusions

The paper discusses the applicability of ultrasonic velocity ratio ($R_{UV} = V_T/V_L$) for materials characterization applications. It has been demonstrated that R_{UV} increases with increasing ultrasonic velocities in pore-free isotropic solid materials. A new polynomial correlation is established between R_{UV} and shear wave velocity for isotropic solid materials. For specific alloy systems, the behavior can be described by a linear correlation due to a limited range of variations. The application of R_{UV} for in-situ assessment of degradation in mechanical properties is demonstrated with a typical example of assessment of service induced degradation in Inconel 625 ammonia crack tubes. Further, the opposite behavior (increase in R_{UV} with decreasing ultrasonic velocities) observed in porous ceramics or materials with microcracks, is demonstrated in boiler water tubes subjected to hydrogen damage and a stainless steel with inter-granular corrosion damage. The present study demonstrates that R_{UV} can be used as an effective tool for in-situ materials characterization applications due to its inherent advantage of thickness independent measurement.

Acknowledgement

The author is thankful to the colleagues of Ultrasonic Measurements Section, NDE Division for their help and many useful discussions. Author is also thankful to Dr. B. Purnachandra Rao, Head, NDE Division; Dr. G. Amarendra, Director, Metallurgy and Materials Group and Dr. A.K. Bhaduri, Director, IGCAR for encouragements and support.

References

[1] A. Viswanath, Anish Kumar, T. Jayakumar, B. P. C. Rao: Ultrasonic characterization of microstructural changes in Ti-10V-4.5 Fe-1.5 Al β-titanium alloy. Metall Mater Trans A **46** (2015) 3393–3405.

[2] R. Raghavan, V.V. Shastry, Anish Kumar, T. Jayakumar, U. Ramamurty: Toughness of as-cast and partially crystallized composites of a bulk metallic glass. Intermetallics **17** (2009) 835–839.

[3] Anish Kumar, T. Jayakumar, Baldev Raj, D. Banerjee: A new methodology for identification of β-transus temperature in $\alpha+\beta$ and β-titanium alloys using ultrasonic velocity measurement. Philos Mag **88** (2008) 327–338.

[4] K. V. Rajkumar, Anish Kumar, T. Jayakumar, Baldev Raj, K. K. Ray: Characterization of aging behavior in M250 grade maraging steel using ultrasonic measurements. Metall Mater Trans A **38A** (2007) 236–243.

[5] Anish Kumar, K.V. Rajkumar, T. Jayakumar, Baldev Raj, B. Mishra: Ultrasonic measurements for in-service assessment of wrought Inconel 625 cracker tubes of heavy water plants. J Nucl Mater **350** (2006) 284–292.

[6] Anish Kumar, T. Jayakumar, Baldev Raj, K. K. Ray: Correlation between ultrasonic shear wave velocity and Poisson's ratio for isotropic solid materials. Acta Mater **51** (2003) 2417–2426.

[7] Anish Kumar, T. Jayakumar, Baldev Raj, K. K. Ray: Characterization of solutionizing behaviour in V_T14 titanium alloy using ultrasonic velocity and attenuation Measurements. Mat. Sci. Eng, A **360** (2003) 58–64.

[8] Y. M. Cheong, D.-H. Lee, S.-J. Kim, Y.-S. Kim: Nondestructive detection of hydride blister in PHWR pressure tube using an ultrasonic velocity ratio method. J. Korean Nucl Soc **35** (2003) 369–377.

[9] Anish Kumar, Vani Shankar, K. Bhanu Sankara Rao, T. Jayakumar, Baldev Raj: Correlation of microstructure and mechanical properties with ultrasonic velocity in the nickel base superalloy Inconel 625. Philos Mag A **82** (2002) 2529–2542.

[10] Anish Kumar, K. Laha, T. Jayakumar, K. Bhanu Sankara Rao, Baldev Raj: Comprehensive microstructural characterization in modified 9Cr-1Mo ferritic steel by ultrasonics. Metall Mater Trans A **33** (2002) 1617–1627.

[11] Li Min Wang, W. H. Wang, R. J. Wang, Z. J. Zhan, D. Y. Dai, L. L. Sun, W. K. Wang: Ultrasonic investigation of Pd39Ni10Cu30P21 bulk metallic glass upon crystallization. Appl Phys Lett **77** (2000) 1147–1149.

[12] A. A. Hesham, Ahmed E. I. Sayed: Ultrasonic properties of ENR-EPDM rubber blends. Polym Bull **50** (2003) 115–122.

[13] Chengbo Yu, Shaocheng Ji, Qi Li: Effects of porosity on seismic velocities, elastic moduli and Poisson's ratios of solid materials and rocks. J Rock Mechan Geotech Eng **8** (2016) 35–49.

[14] J. B. Spicer, L. R. Olasov, F. W. Zeng, K. Han, N. C. Gallego, C. I. Contescu: Laser ultrasonic assessment of the effects of porosity and microcracking on the elastic moduli of nuclear graphites, J of Nucl Mater **471** (2016) 80–91.

[15] I. Ozkan, Z. Yayla: Evaluation of correlation between physical properties and ultrasonic pulse velocity of fired clay samples. Ultrasonics **66** (2016) 4–10.

[16] M. W. Lee: Velocity ratio and its application to predicting velocities, Geological Survey (U.S.), Volume 2197 of U.S. Geological Survey bulletin, 2003, U.S. Department of the Interior, U.S. Geological Survey. https://books.google.co.in/books?id=l0lrAQAACAAJ,

[17] F. Lofaj, G. V. Blessing, S. M. Wiederhorn: Ultrasonic velocity technique for nondestructive quantification of elastic moduli degradation during creep in silicon nitride. J Am Ceram Soc **86** (2003) 817–22.

[18] R. W. Rice: Porosity of Ceramics. Marcel Dekker Inc., Switzerland, 1998.

[19] J. P. Panakkal: Longitudinal ultrasonic velocity in plutonium-uranium carbide (0.7Pu-0.3U)C pellets. J of Nucl Mater **172** (1990) 135–137.

[20] T. Watanabe, Y. Hasegawa, K. Kato: Ultrasonic velocity ratio method for detecting and evaluating hydrogen damage in steels, Corrosion monitoring in industrial plants using nondestructive testing and electrochemical methods, ASTM STP 908, G.C. Moran and P. Labine Eds., American Society for Testing and Materials, Philadelphia, 1986, 153–164.

[21] W. Koister, H. Franz. Metall Rev. **6** (1961) 1–55.

[22] N. Jothilakshmi, P. P. Nanekar, V. Kain: Assessment of intergranular corrosion attack in austenitic stainless steel using ultrasonic measurements. Corrosion **69** (2013) 388–395.

[23] C. E. Morris, J. C. Jamieson, F. L. Yarger: Ultrasonic measurements at elevated pressures (9 GPa) to determine Poisson's ratio and other elastic moduli of NaCl and NaF. J Appl Phys **47** (1976) 3979–3986.

[24] S. Chaki, G. Corneloup, I. Lillamand, H. Walaszek: Combination of longitudinal and transverse ultrasonic waves for in situ control of the tightening of bolts. J Press Vessel Tech. **129** (2007) 383–390.

[25] H. Yasui, H. Tanaka, I. Fujii, K. Kawashima: Acoustoelastic axial stress measurement of short bolts with longitudinal and transverse waves, Review of Progress in Quantitative Nondestructive Evaluation, Vol 18. D. O. Thompson, D. E. Chimenti (Eds.), Plenum Press, New York, 1999, 1903–1909.

[26] I. Fujii, K. Kawashima: Digital measurement of ultrasonic velocity. Review of Progress in Quantitative Nondestructive Evaluation, Vol 14. D. O.Thompson, D. E. Chimenti (Eds.), Plenum Press, New York, 1995, 203–209.

[27] D. R. Hull, H. E. Kautz, A. Vary: Measurement of ultrasonic velocity using phase-slope and cross-correlation methods. Mater Eval **43** (1985) 1455–1460.

[28] P. Palanichamy, C. V. Subramanian, Baldev Raj: Couplant correction for ultrasonic measurements. British J NDT **31** (1989) 78–80.

[29] H. M. Ledbetter: Elastic Properties, Materials at low temperatures. R. P. Reed, A. F. Clark (Eds.), American Soc. for Metals, Metals Park, Ohio 44073, 1983, 1–45.

[30] R. Lakes. Science **235** (1987) 1038–1040.